# Satellite-based climatology of Mediterranean cloud systems and their association with large-scale circulation.

Jean-Pierre Chaboureau, C. Claud

# Satellite-based climatology of Mediterranean cloud systems and their association with large-scale circulation

Jean-Pierre Chaboureau
Laboratoire d'Aérologie, Observatoire Midi-Pyrénées, Université Paul Sabatier and CNRS, Toulouse, France

Chantal Claud
Laboratoire de Météorologie Dynamique/IPSL, École Polytechnique, Palaiseau, France

Received 2 July 2005; revised 28 October 2005; accepted 15 November 2005; published 11 January 2006.

[1] The variability of Mediterranean cloud systems is investigated using 8.5 years (from January 1987 to June 1995) of TIROS-N Operational Vertical Sounder (TOVS) observations acquired aboard the National Oceanic and Atmospheric Administration (NOAA) series of operational polar satellites. Cloud systems and troughs are automatically detected with the retrievals of the cloud top pressure (CTP) and the temperature of lower stratosphere (TLS). Observed cloud systems have a typical size of few hundred kilometres with a larger occurrence between March and October. A threefold cloud system typology reveals the presence of an upper-level anomaly for about 30% of the cloud systems in winter, 26% in spring and 7% in autumn (but 23% in October). During summer, in contrast, the forcing is very likely local, and according to the composite analysis, weakly related to upper-level anomaly. During the cold seasons (15 October to 15 April), more cloud systems are found during negative North Atlantic Oscillation (NAO) phase when the north Atlantic storm track takes its southernmost position. Consistently, more systems are observed during the Greenland Anticyclone and the Atlantic Ridge regimes, compared to the Zonal and Blocking regimes. Finally, severe precipitation events over the Alpine region are associated with a warm TLS anomaly upstream the cloud system, showing once more the impact of the upper levels on the weather over this area.

**Citation:** Chaboureau, J.-P., and C. Claud (2006), Satellite-based climatology of Mediterranean cloud systems and their association with large-scale circulation, *J. Geophys. Res.*, *111*, D01102, doi:10.1029/2005JD006460.

## 1. Introduction

[2] The Mediterranean basin is a region known for its cyclonic activity. Due to its specific orography (the Mediterranean Sea is surrounded by an almost continuous barrier of mountains) and the high sea surface temperature, the distribution of cyclones over this area is complex, as confirmed by a pioneer subjective analysis [*Petterssen*, 1956]. There have been since then several studies aiming at characterizing the sub-areas of cyclogenesis, the seasonality and the generation mechanisms of Mediterranean systems, which all rely on reanalyses and/or simulations. *Alpert et al.* [1990a] first and then *Trigo et al.* [1999], using European Center for Medium-Range Weather Forecasts 15-year reanalysis (ERA-15), showed that the characteristic time and space scales of cyclones in the Mediterranean region are smaller than in the Atlantic, with over 65% of cyclones having a radius less than 550 km and an average time of about 28 hours. Larger systems were found in the western Mediterranean. *Picornell et al.* [2001] used High Resolution Limited Area Modelling (HIRLAM) 0.5° resolution fields to study mainly short-living cyclones and found that most systems have a radius between 150 and 300 km. *Maheras et al.* [2001], using 40 years of the National Centers for Environmental Prediction (NCEP) National Center for Atmospheric Research (NCAR) data, studied seasonal and diurnal variations of cyclones occurrence, as well as the trend in cyclone frequency. All these studies (plus earlier ones) indicate that there are different generation areas, different cyclone types and generation mechanisms and also a strong seasonal and even inter-monthly variability [*Alpert et al.*, 1990a, 1990b; *Trigo et al.*, 1999]. Also, a number of cyclones have a null or even negative deepening rate, which means that they originated in other regions and just cross the Mediterranean during their attenuation phase. As mentioned before, several mechanisms play a role like orography, latent heat release at the sea surface (local forcing) but the intensity of the cyclogenetic activity is to a large extent controlled by large-scale processes over Europe and especially those characterized by mid and upper-tropospheric southward air mass intrusions and tropopause foldings, which are often associated with potential vorticity (PV) structures and jet streaks [e.g., *Massacand et al.*, 1998; *Buzzi and Foschini*, 2000; *Stein et al.*, 2000; *Liniger and Davies*, 2003].


0148-0227/06/2005JD006460

[3] Instead of considering reanalysis where cyclones are usually detected by identifying 1000 hPa height minima, an alternative source of data is used here in order to study both the climatological features and the associations with large scale patterns. It consists of satellite data as recently shown by *Chaboureau and Claud* [2003] who have investigated the wintertime variability of large precipitating weather systems over the North Atlantic Ocean. Their study was based on the signature of the storms on the water budget (clouds and precipitation) as observed from the TIROS-N Operational Vertical Sounder (TOVS) on board National Oceanic and Atmospheric Administration (NOAA) satellites. They showed that three retrieved fields, the temperature of the lower stratosphere (TLS), the cloud top pressure (CTP), and a precipitation index ΔMSU, can be used to characterize the intraseasonal variability. Moreover, a composite study of the weather systems with the largest precipitation signature suggested a relationship between types of precipitating systems and low frequency variability described by the North Atlantic Oscillation (NAO).

[4] The objective of this study is to adapt this work to the Mediterranean cyclones, that is, to provide a typology of cloud systems for each season, to determine the proportion of lows for which the dynamics is dominated by the upper-level situation and to examine the potential relationship between individual cloud systems and low-frequency variability. In addition, the links between precipitation and the upper-level configuration will be studied for the Alpine region, for which a daily precipitation climatology exists. Section 2 presents the data and the classification method. Section 3 describes the cloud system climatology obtained for the 8.5 years. Section 4 details the cloud-system typology season by season. Section 5 explores the link between the cloud system variability and the Atlantic large-scale circulation. Section 6 concentrates on the Alpine region. Section 7 provides a conclusion to the study.

## 2. Data and Methodology

### 2.1. Satellite Data

[5] Observations used for this study are from NOAA-10 and NOAA-12 satellites and cover 8.5 years from 1 January 1987 to 30 June 1995. The TOVS radiometer, which flies on board the NOAA satellites, mainly consists of two instruments: HIRS-2 (High resolution Infrared Radiation Sounder) and MSU (Microwave Sounding Unit). HIRS-2 is a radiometer with 19 channels in the infrared band and one in the visible band and its spatial resolution is about 17 km at nadir. MSU is a four-channel passive microwave radiometer for which the horizontal resolution is ranging from 110 km at nadir to 323 km at the edges of the swath. The raw TOVS data have been converted into atmospheric parameters using the Improved Initialization Inversion algorithm [*Chédin et al.*, 1985; *Scott et al.*, 1999]. Among a large number of variables, this physico-statistical method, relying on pattern recognition approach, determines the temperature of the lower stratosphere and the cloud top pressure. All these variables are retrieved at a spatial resolution of 100 km by 100 km every 12 hours at best, that is at 7:30 and 19:30 local time.

[6] The temperature of lower stratosphere (TLS) is used to describe the thermal structures at the tropopause level [*Fourrié et al.*, 2000]. TLS is obtained through a combination of brightness temperatures from five TOVS channels (HIRS 2 and 3; MSU 2, 3, and 4) weighted by a set of regression coefficients. These TOVS channels are the most sensitive to the temperature around the tropopause. While MSU3 plays the major role, the other channels are also significant. As a consequence, TLS fields show more variability than the raw MSU3 data alone. As shown through quantitative comparisons with model analysis, TLS is a good indicator of the averaged temperature between the 4 and 8 PVU (potential vorticity unit, 1 PVU = $10^{-6}$ K m$^2$ s$^{-1}$ kg$^{-1}$) levels (i.e., in the layer 1–4.5 km above the tropopause). In particular, warm anomalies of TLS can be used to detect upper level precursors. Moreover, TLS fields allow detecting other upper level structures such as troughs, ridges, and tropopause breaks along the cyclonic shear side of an upper level jet [*Fourrié et al.*, 2000, 2003].

[7] In the 3I algorithm, clouds are detected at the HIRS spatial resolution (18 km at nadir) by a succession of 7 (night)/8 (day) threshold tests, which depend on the simultaneous MSU radiance measurements probing through clouds. Cloud parameters are determined from the radiances averaged over all cloudy HIRS pixels within the 3I box, assuming a single, homogeneous cloud layer. The average cloud top pressure (CTP) and the effective cloud amount are obtained by a weighted-$\chi^2$ method from four 15 μm $CO_2$ band radiances and the 11 μm atmospheric window radiance (HIRS 4 to 8) [*Stubenrauch et al.*, 1999a]. The empirical weights reflect the usefulness of a spectral channel at a cloud level for the determination of the effective cloud amount. A cloud cover fraction is also determined as the fraction of cloudy HIRS pixels in each grid box. The 3I cloud parameters have been evaluated on a global scale [*Stubenrauch et al.*, 1999b] by comparison with time-space collocated, reprocessed ISCCP cloud parameters. The remaining discrepancies with ISCCP can be explained by differences in cloud detection sensitivity, differences in the atmospheric temperatures profiles used, and by inhomogeneous or partly cloudy fields.

### 2.2. Classification Method

[8] In [*Chaboureau and Claud*, 2003], only weather systems with both a large precipitation signature and a high level cloud cover were considered. These precipitating events were defined by areas covering more than 200,000 km$^2$ (corresponding to an equivalent radius of 250 km) with normalized ΔMSU less than 16 K (a threshold indicator of rain) and with a CTP less than 400 hPa. In the case of the Mediterranean Basin, the precipitation index cannot be used: as a matter of fact, continental surfaces and precipitating hydrometeors have similar microwave emissivities, which prevents from discriminating between them. Therefore, the selection is done only on the cloud level. Considering systems with CTP less than 400 hPa means that shallow systems are not included in our study. In contrast with studies quoted above, there is no tracking procedure, which implies that a single system can be detected several times on subsequent orbits. In addition, we consider the area between 30°N–48°N and 10°W–45°E, encompassing all the Mediterranean Sea and the surrounding regions.

[9] The variability of the selected cloud systems is investigated using a composite method. TLS and CTP fields

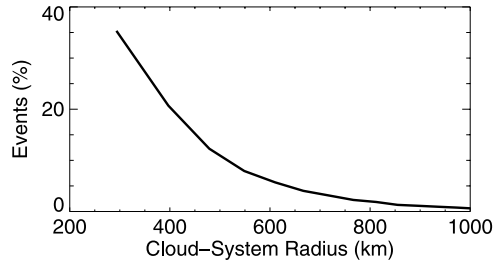


**Figure 1.** Frequency distribution of the cloud-system radius.

are extracted in a square of 3600 km side length for which the Y axis is toward the north. To enlarge the view upstream of the cloud event (i.e. to the west), the box is shifted 900 km to the east from the geometric centre of the box. A principal component analysis (PCA) is then performed on the normalized fields of TLS and CTP. The latter are projected onto the components of the first eigenvectors which represent the larger variance. So the PCA yields the ability to select only the pertinent information, that is, the field of variation around their average, and the large-scale structures as described by the first eigenvectors. The mean fields of TLS and CTP, and the small-scale structures are therefore filtered out. Here, we have chosen to retain the first components that represent 45% of the total variance. Then, the components kept are clustered using an ascending hierarchical classification, which minimizes the intraclass variance: each case is then included in a class. Finally, composites within each class are build from averaging the original fields (i.e., not the filtered fields described by the first eigenvectors). This yields realistic structures as illustrated below.

## 3. Cloud System Climatology

[10] Over the 102 months, a total of 9906 cloud systems have been identified, without any particular interannual variation. With two observations per day, this leaves about 48 systems per month. 35% of the cloud systems have an equivalent radius of 250 km, and over 70% less than 550 km (Figure 1). This result is in agreement with the 65% of cyclones having a maximum radius less than 550 km obtained by *Trigo et al.* [1999] using reanalyses. This confirms that most of the Mediterranean lows are within the mesoscale, in contrast to synoptic North Atlantic cloud systems with typical sizes lying between 1000 and 3000 km [*Chaboureau and Claud*, 2003].

[11] The number of selected cloud systems per grid point for the whole period is shown in Figure 2. The cloud systems are found in preferential areas: The western North Africa, the eastern coast of the Iberian Peninsula, the Balearic Islands, the Gulf of Genoa, southern Italy, the Aegean Sea, and Cyprus. However, this geographical distribution is more spread than the map of the first cyclone detections shown by *Trigo et al.* [1999] or those of the cyclonic occurrence by *Maheras et al.* [2001]. Two reasons can explain this difference. First, in contrast to these studies, the present analysis groups not only cyclones, but also fronts and convective systems. Moreover, since we have no tracking procedure, this map does not correspond to the first detection but to the cumulated number of detections during the whole life-cycle of the cyclones. Second, less cyclones are found over the eastern Black Sea, and the Middle East but for this latter region, *Trigo et al.* [1999] mention that the number is probably overestimated due to being near the domain's boundary. Concerning the Black Sea, differences might be due to the fact that satellite passes are at 7:30 and 19:30 local time while the frequency of cyclones increases over this area during the night, especially in summer [*Maheras et al.*, 2001], which corresponds to a peak of activity.

[12] For a better geographical and temporal characterisation of the systems, the domain has been partitioned off according to the latitude of 36°N and the longitude of 20°E yielding four regions (SW, NW, SE, NE). Figure 3 presents the monthly fraction of cloud systems for the 8.5 years. Overall, the fraction is the largest between March and October with local maxima in May and in October. The fraction of cloud systems is during the whole year larger in the western part of the Mediterranean basin compared to the eastern part. This is due to a peak of activity in May and June over the SW region (Sahara). Also a higher activity is found in the NW region, with a maximum in March and August, over the Balearic Islands and the Iberian Peninsula, respectively. The cloud system occurrence in the SE region

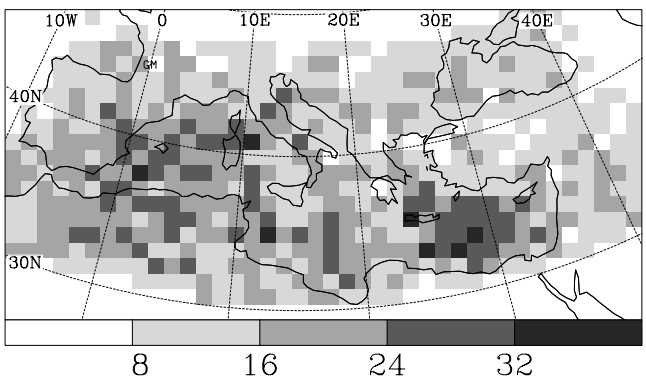


**Figure 2.** Number of selected cloud systems per grid point for the full 8.5-year period.

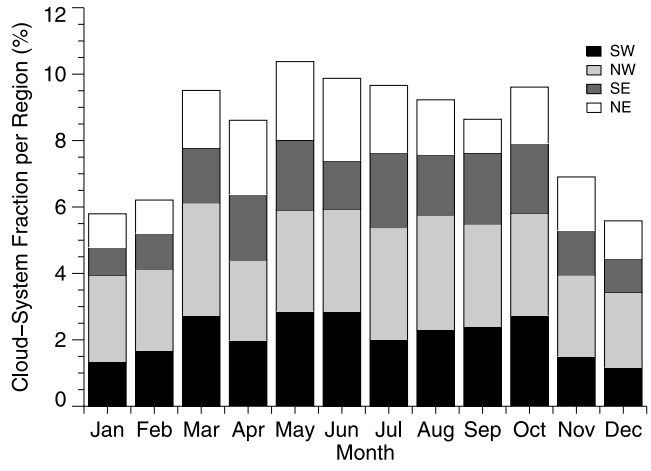


**Figure 3.** Fraction of cloud systems per month for different geographical areas (see text).

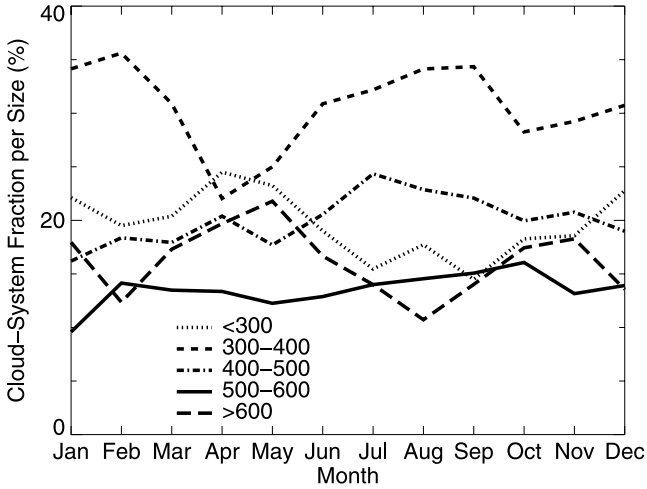


**Figure 4.** Fraction of cloud systems per month for different categories of cloud-system radius.

(Cyprus and Middle East) is maximum between April and October with a peak in July. In the NE region, the maximum activity peaks between April and July.

[13] Moreover, the monthly distribution is shown according to different size classes depending on the equivalent radius (Figure 4). Around 35% of the systems fall into the category 300–400 km, independently of the month with the exception of April. Systems within categories 300–400 km and 400–500 km are more frequent in spring and summer. On the other hand systems within categories less than 300 km and larger than 600 km occur preferentially during spring, but present also a peak in October.

## 4. Threefold Seasonal Cloud System Typology

[14] A typology of these 9906 cloud systems with their TLS field is now presented. For the sake of simplicity, a classification with only three classes is shown here. The partition into three classes gives however some indications on the way the cloud systems can develop. Furthermore, the composite method is applied separately to the four seasons. Studies by *Trigo et al.* [1999, 2002], among others, have nevertheless shown that the Mediterranean weather is characterized by three distinct seasons, namely winter (DJF), spring (MAM), and summer (JJA), while autumn months (SON) more easily fall either into the (late) summer or (early) winter categories. Our results suggest that fall is a season in itself. October follows its own peculiar behavior, and as such, it has been considered alone.

### 4.1. Winter

[15] A total of 1742 cloud systems are selected in winter. Figure 5 shows the resulting composite fields and the number of cases for each class which lies between 274 and 522 cases. A large variability between the composites is observed according to the orientation of the cloud system, its extent (as seen by CTP less than 560 hPa), the meridional tilting and the magnitude of the TLS field, and the cloud

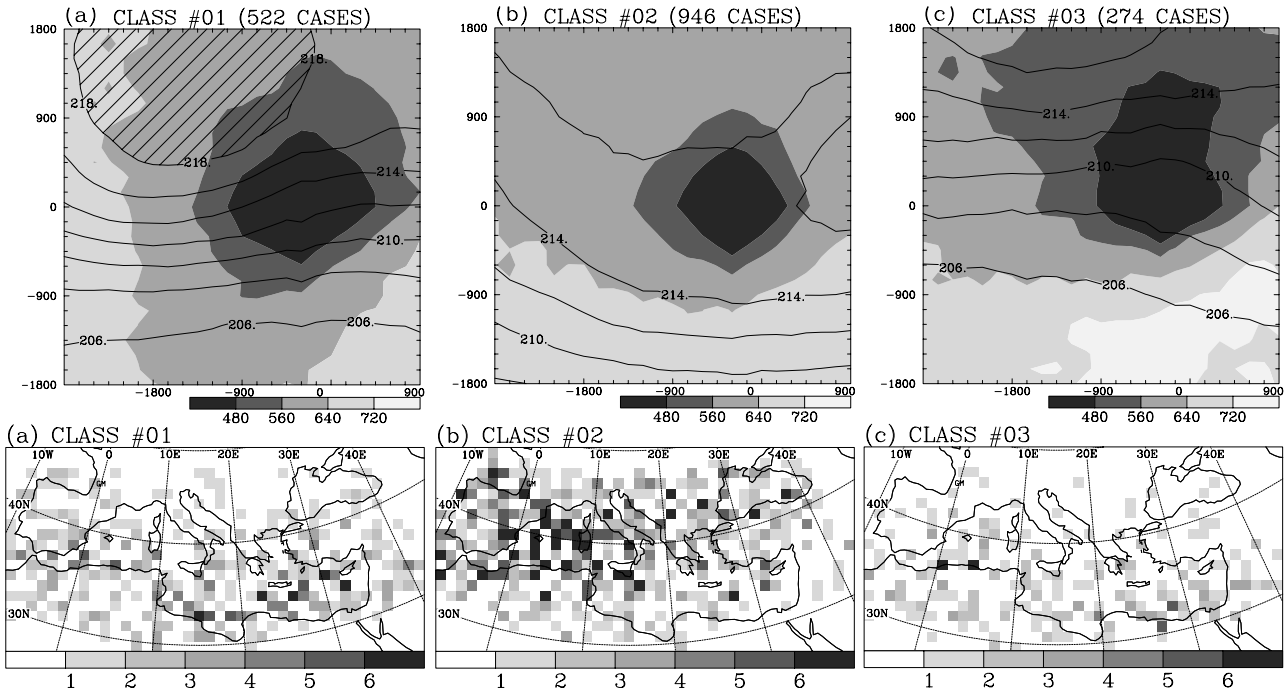


**Figure 5.** Winter. (top) Composite views of the three classes resulting from the hierarchical classification. The ordinate (abscissa) of the coordinate system corresponds to northward (westward) displacements in kilometers from the cloud system center located at (0,0) km. The shading indicates CTP every 80 hPa, the white solid line CTP less than 400 hPa, the black contours TLS every 2 K, and the hatched patterns TLS over 218 K. (bottom) Number of cloud systems selected per grid point for each of the three classes.

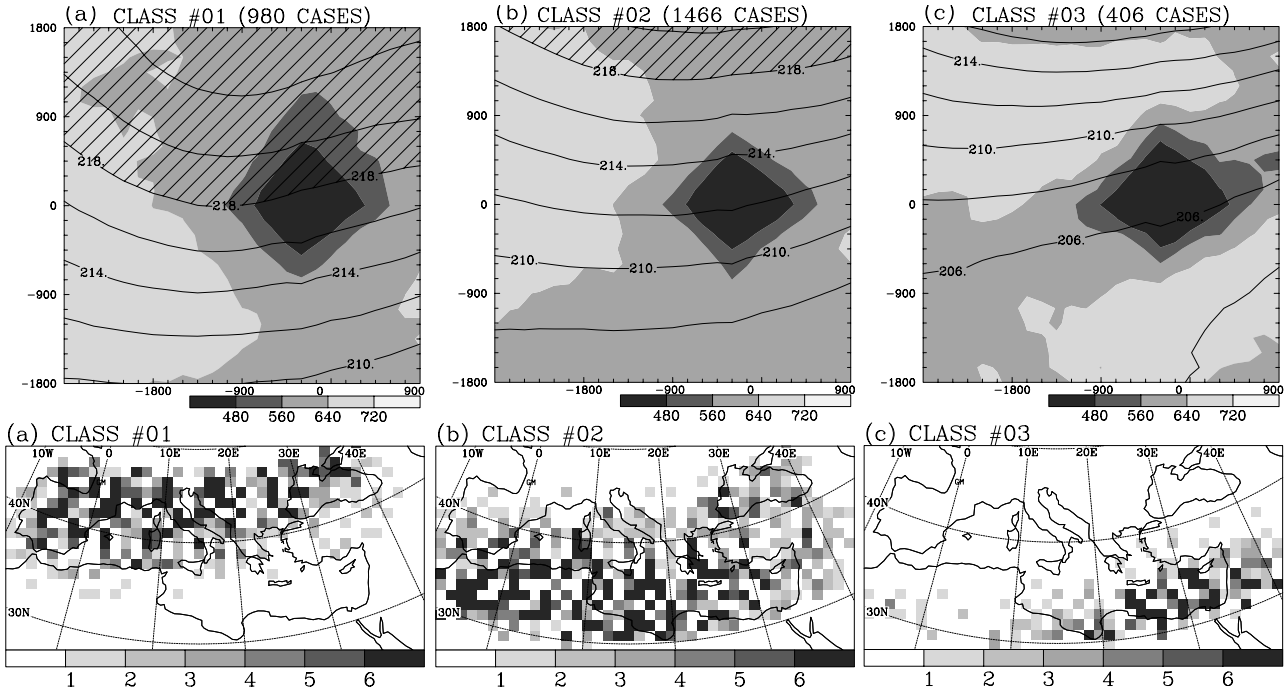


**Figure 6.** Same as Figure 5, but for summer.

system location relative to the TLS gradient. Class 1 is characterized by a warm TLS pattern upstream the cloud system. These cloud systems have a south-north orientation with a slight cyclonic curvature and are relatively large. This configuration suggests that these systems are triggered by an upper-level trough located upstream, as also observed in the north Atlantic [*Chaboureau and Claud*, 2003]. They represent about 30% of the whole wintertime systems and are found preferentially over the southern Mediterranean Sea. In contrast, cloud systems from class 2 are found mostly in the western part of the domain and to a lesser extent to the northeast. The composite high-cloud cover is rather compact and the associated TLS field presents a more zonal orientation with a larger gradient to the south. These systems are associated with a trough located over Europe and represent more than 54% of the cases. Finally, class 3 groups systems that occur preferentially in the southern part of the domain, associated with subtropical air intrusions. Clouds are pointing towards the north and are embedded in a weak TLS gradient.

### 4.2. Summer

[16] In summer a total of 2852 cloud systems are selected. The composite high-cloud field, as seen by CTP less than 560 hPa, is compact whatever the class (Figure 6). This compactness can been partly explained by the larger occurrence of cloud systems within categories 300–400 km and 400–500 km in summer compared to the other seasons (Figure 4). On the other hand, all the TLS composite fields present a zonal gradient. However, they differ from each other by the TLS value, i.e. the larger the TLS, the northernmost the class. The absence of any strong meridional pattern in the TLS field indicates a weak influence of tropopause anomalies, such as troughs or cut-off lows, on the cloud system development. As expected, this hints that summertime cloud systems are forced by more local (mesoscale) factors (land-sea contrast and topography) than by synoptic ones. Note also that a large number of cloud systems are found over land, in contrast to the location of the wintertime cloud systems.

### 4.3. Spring

[17] The composite analysis done on the 2822 cloud systems selected in spring is presented in Figure 7. Class 1, which represents 26% of the total selected cloud systems, displays a composite cloud field oriented north-south with a slight cyclonic tilting to the east of a warm TLS pattern, and mostly occurs in the north of the Basin. Cloud systems from classes 2 and 3 are embedded in a symmetrical zonal gradient and are found in the southern part of the domain. These springtime composite fields of classes 2 and 3 present some similarities to those found in autumn, as discussed below.

### 4.4. Autumn

[18] The selection results in 2492 cloud systems for the fall season (Figure 8). Class 1 represents only 7% of the cases but very likely corresponds to extreme cases of precipitation and floods. It corresponds to the typical configuration expected for baroclinic interaction (cloud field oriented north-south with a slight cyclonic tilting to the east of a warm TLS pattern) that mostly occurs in the northern part of the Mediterranean Basin, and preferentially over land. The TLS pattern presents the warmest anomaly (TLS larger than 220 K) of all the seasonal composites. Class 2 essentially groups elements from the western part, while class 3 corresponds to southernmost cases. They represent about 43% and 50% of the cases, respectively. They show similar composite cloud fields embedded in a zonal TLS gradient. Class 2 displays a slightly larger TLS

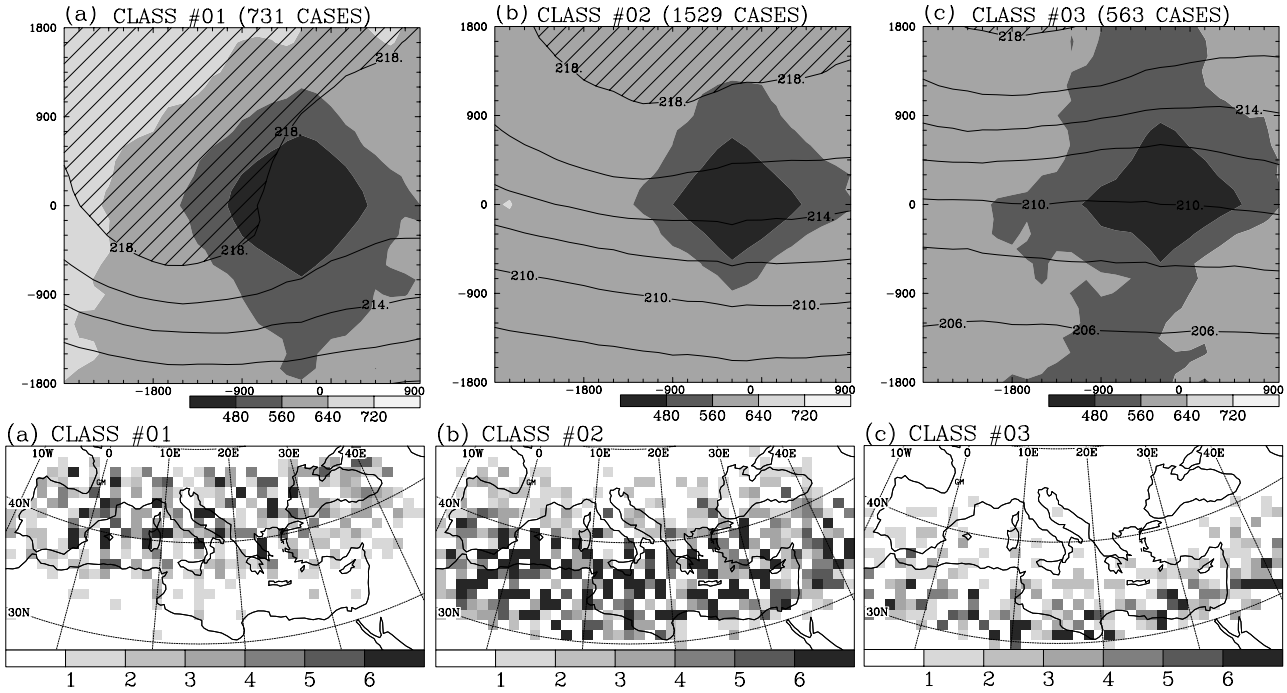


**Figure 7.** Same as Figure 5, but for spring.

gradient than class 3. As such, cloud systems from class 2 are found more to the north than those of class 3.

### 4.5. Summary

[19] In conclusion, the analysis shows that during winter, for about 30% of the cloud systems, the dynamics is dominated by an upper PV anomaly. This rate decreases to 26% in spring and only 7% in autumn. However, it must be noted that if the composite analysis is restricted to October (not shown), then 23% of the systems display a tropopause anomaly. In addition, these events in autumn are likely to be severe, since these are the only cases where the TLS values are larger than 220 K. Finally, in contrast, during summer, the forcing is very likely local,

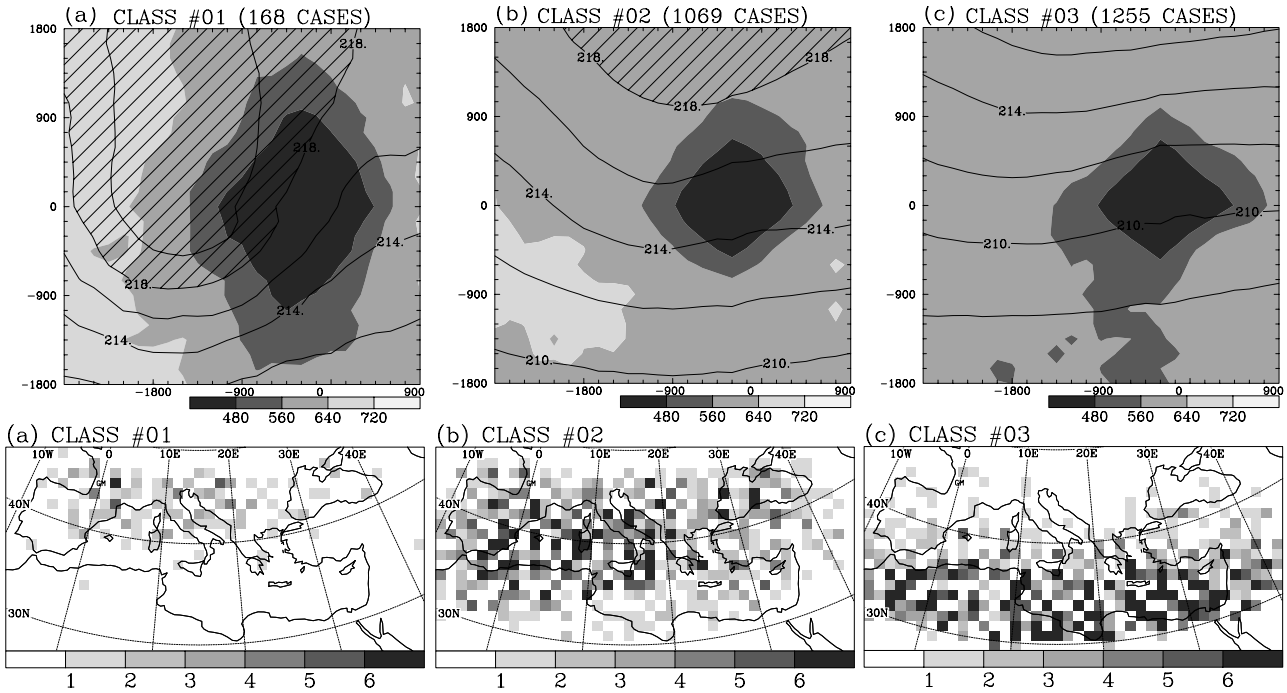


**Figure 8.** Same as Figure 5, but for autumn.

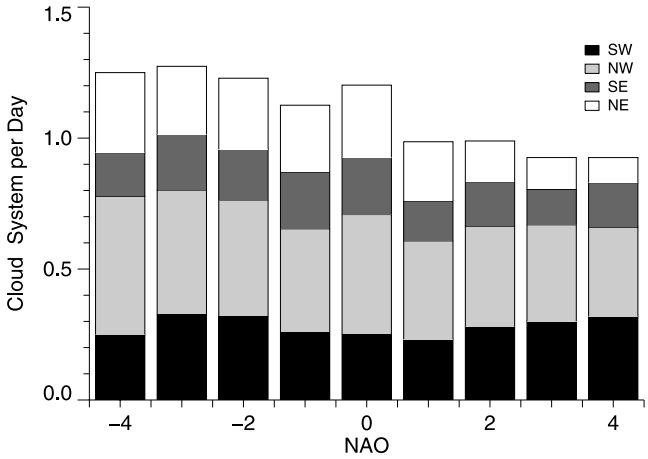


**Figure 9.** Number of cloud systems per day according to the NAO during the cold season (15 October to 15 April) for different geographical areas.

and according to this composite analysis, not related to PV anomaly.

## 5. Cloud System Variability During Cold Season and Its Links With Atlantic Large-Scale Circulations

[20] During winter, or more generally the cold season (from 15 October to 15 April), the Mediterranean Basin is primarily influenced by the tail end of the Atlantic storm tracks [e.g., *Hurrell*, 1995; *Quadrelli et al.*, 2001]. The low-frequency variability in the Northern Atlantic Basin is often described by the leading empirical orthogonal function of the sea level pressure (SLP) or the geopotential field which yields the North Atlantic Oscillation (NAO). The index used here is the daily NAO index generated by the NOAA Climate Prediction Center. After *Hurrell* [1995], during the positive NAO phase, precipitating systems follow a more southwest-to-northeast Atlantic storm track. Conversely, during the negative NAO phase, the precipitating systems follow a west-east storm track. Figure 9 presents the number of cloud systems per day vs. NAO (i.e. the number of detected cloud systems over the number of days within the considered NAO bin) for the cold season. As expected, a larger number of cloud systems are found for negative NAO values, especially in the NE area.

[21] The interannual variability in the North Atlantic domain can also be examined through non-linear approaches such as cluster analysis. This yields the concept of weather regime, a dynamically equilibrated pattern corresponding to quasi-steady persistent weather as defined by *Vautard et al.* [1988]. A regime identification based on the 700 hPa geopotential field of the four-daily analyses produced by European Center for Medium-Range Weather Forecasts (ECMWF) performed by *Ayrault et al.* [1995] is considered. Four weather regimes are identified: the Zonal (ZO), Blocking (BL), Greenland Anticyclone (GA), and Atlantic ridge (AR) regimes. The ZO regime corresponds to a maximum eastward penetration of the zonal jet, associated with a low centred over northern Europe extending upstream to Greenland. The BL is characterized by the jet confined to the western part of the Atlantic, bringing easterlies over Western Europe. The GA regime corresponds to an anticyclone over Greenland and the polar jet moved southward by reference to its ZO regime position, almost in continuity with the African subtropical jet. This gives a zonally symmetric pattern to its southern part. The AR regime is characterized by a ridge over the mid-eastern Atlantic, bringing over Europe moist cold air advected from the north Atlantic. In contrast to the typical NAO pattern identified through linear approaches, some spatial asymmetries are found, in particular a significant eastward displacement towards Europe for the ZO regime (that mimics the positive NAO phase) compared to the GA regime (corresponding to the negative NAO phase) [*Cassou et al.*, 2004].

[22] The cloud system geographical distribution for each regime is shown in Figure 10. During the ZO regime, a vast majority of the cloud systems is found between 10°W and 20°E. During the BL regime, the cloud systems are also more frequent in the western part of the domain, more particularly over the Balearic Islands and the Gulf of Genoa. During the GA regime, again, cloud systems occur more frequently in the western part of the Basin. In contrast, the preferential areas during the AR regime are almost everywhere in the domain, with a high concentration around Cyprus. However, the cloud system distributions shown in Figure 10 also depend upon the occurrence of the Atlantic weather regimes. During the period studied here, the occurrence is 36% for the ZO regime, 24% for BL, 14% for GA, and 26% for AR. Therefore, for a similar number of days, more cloud systems are found during the AR regime than the BL one. In a similar way than in Figure 9 for NAO, the number of cloud systems per day for each Atlantic weather regime is shown in Figure 11. During the ZO and BL regimes, less than one cloud system is found while during the GA and AR regimes, more than 1.3 cloud systems are detected. This difference is mainly due to a doubling of detected cloud systems in the NW, SE, and NE regions. This result underscores the influence of the north Atlantic storm track in the Mediterranean domain during the cold season.

[23] Figure 11 also displays the cloud-system distribution per day among different categories of cloud-system radius. During the ZO, GA, and AR regimes, the number of systems with a radius less than 400 km is roughly equivalent to the number of larger systems. Only the BL regime is characterized by a larger fraction of small-scale systems (60%). A study by *Trigo et al.* [2004], based on the 40 years of NCEP-NCAR reanalysis, showed that during blocking episodes, most cyclones have a more south-easterly trajectory, so that there are more systems during blocking episodes than during non-blocking ones. Our results do not confirm this finding. However, a different definition of the weather regimes has been considered in these two studies. In particular, their definition is less conservative for blocking episodes (e.g., four successive days, considered blocked, followed by one non-blocked day and then by five successive blocked days, will lead to a 10-day blocking event), while we have more variability [see, e.g., *Chaboureau*

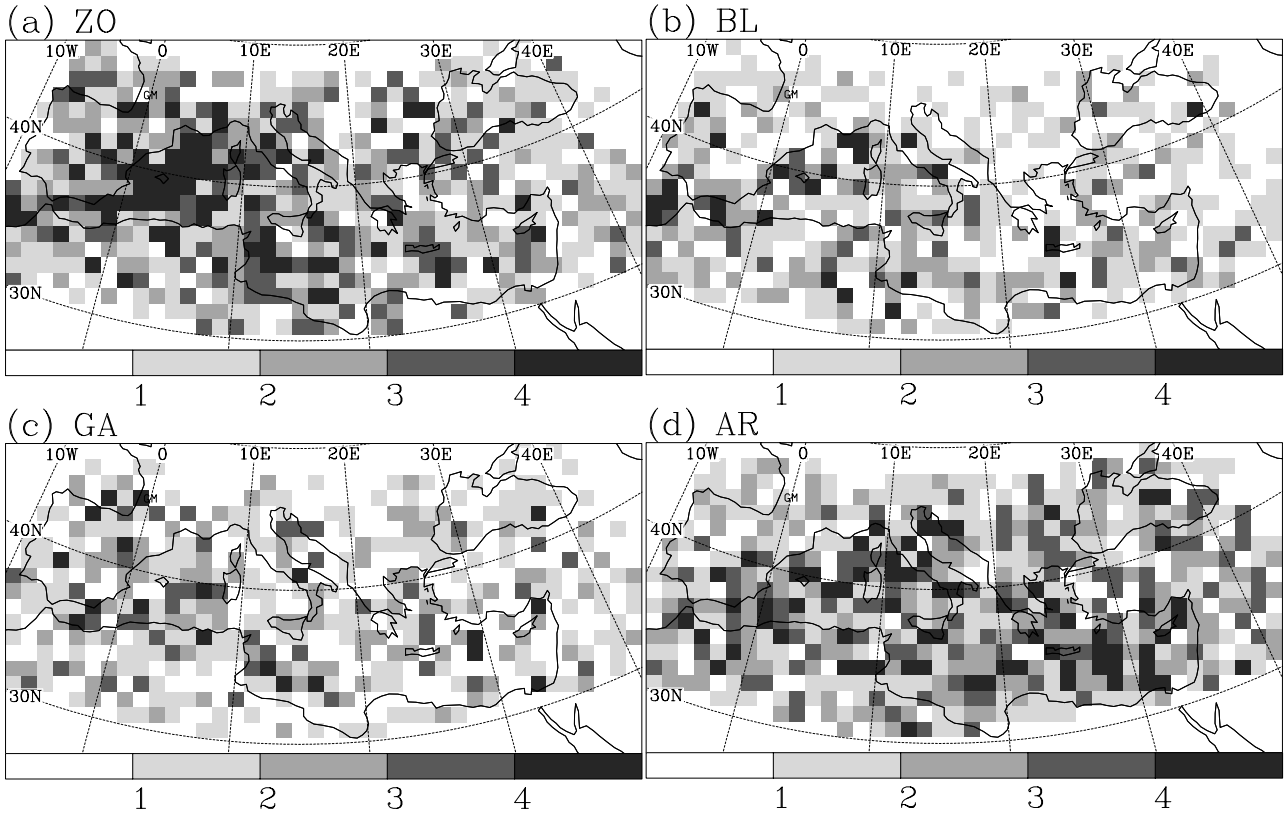


**Figure 10.** Number of cloud systems selected per grid point for each Atlantic weather regime: (a) ZO, (b) BL, (c) GA, and (d) AR during the cold season (15 October to 15 April).

*and Claud*, 2003, Figure 5]. Besides, *Trigo et al.* [2004] consider only DJF months.

## 6. Cloud Systems, Upper-level Forcing, and Precipitation in the Alpine Region

[24] The detection of a warm TLS anomaly upstream of a cloud system suggests a strong upper-level forcing, and potentially more intense precipitation. The daily Alpine precipitation climatology built by *Frei and Schär* [1998] allows examining such a scenario. This climatology consists of gridded daily precipitation analyses, constructed by spatial aggregation of rain gauge observations onto a regular latitude-longitude 0.5° grid-spacing. It covers the Alpine area, between 43°N–49°N and 2°E–17°E. A selection of cloud systems in the same area has been carried out, providing 284 cloud systems for which the composite fields are shown in Figure 12a. On average, a warm TLS pattern is present to the west of the cloud system.

[25] A similar analysis has been performed, restricted to precipitating events larger than 50 mm/day on a grid point of the precipitation climatology (Figure 12b). The threshold of 50 mm/day corresponds to the 90% quantile over where heavy precipitations occurs in three distinct regions: southeast of the Central Massif, south central Alps, and north of Adriatic Sea [*Frei et al.*, 2003]. The 129 selected events occurred mainly in summer and in autumn (Figure 13). Composites show a warmer TLS field to the west of the CTP field, compared to the full set. Cloud systems also have a slightly more elongated shape. This is a typical configuration for baroclinic interaction.

[26] The analysis is done one step further by selecting only the events with rainrate larger than 100 mm/day. This leaves 44 events that occurred mainly in autumn (Figure 13). The associated composite fields resemble those of the previous

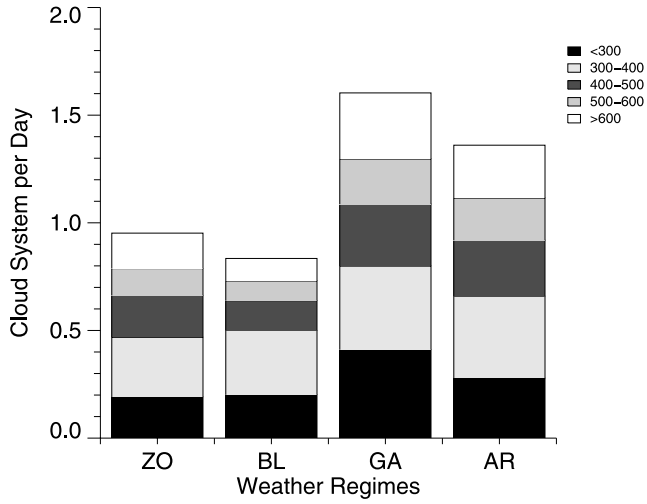


**Figure 11.** Number of cloud systems per day for each Atlantic weather regime during the cold season (15 October to 15 April) for different categories of cloud-system radius.

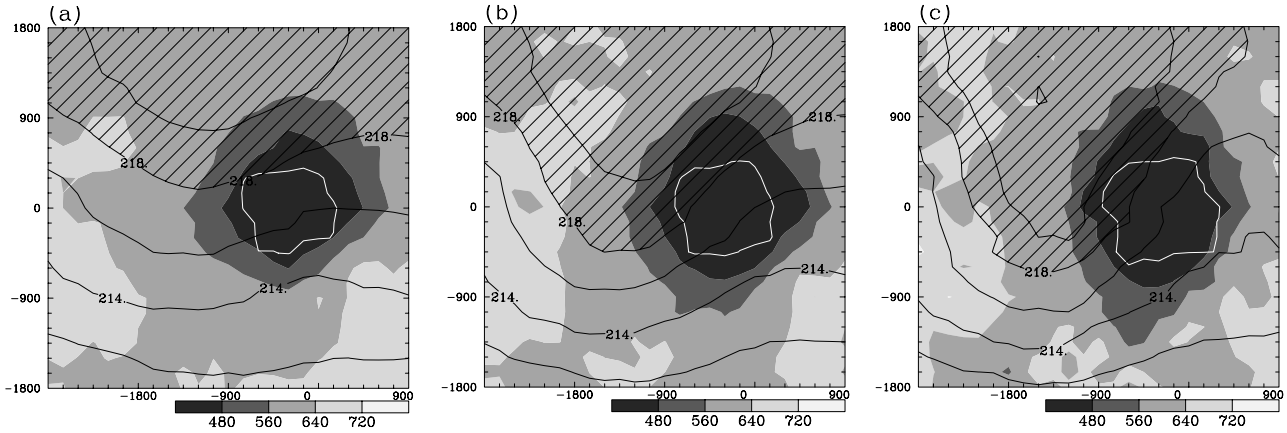


**Figure 12.** Alpine composite fields from (a) the full set, and the sets restricted to events with rainrate higher than (b) 50 mm/day and (c) 100 mm/day within a 50 km grid point. The white line indicates rainrate higher than 1 mm/day.

subset, but with even more elongated cloud system shape and a southernmore warm TLS anomaly (Figure 12c).

## 7. Conclusion

[27] The variability of Mediterranean systems has been investigated using polar satellite data covering the period January 1987–June 1995, in contrast with previous studies which all consider reanalyses. An automatic detection of cloud systems is performed, based on retrievals of cloud top pressure (CTP). Over the 102 months, a total of 9906 cloud systems (storms, fronts, and convective systems) have been identified, with a rather low interannual variation. 35% of the systems have an equivalent radius of 250 km, and over 70% less than 550 km, which is agreement with previous studies, and confirms the fact that over the Mediterranean, most of the lows are within the mesoscale or subsynoptic range, in contrast to North-Atlantic systems. Cloud systems are preferentially detected over western North Africa, the east coast of Spain, the Balearic Islands, the gulf of Genoa, southern Italy, the Aegean Sea and Cyprus. Their most frequent occurrence is between March and October.

[28] Using consistent CTP and TLS fields, a seasonal cloud system typology has been constructed. For the four seasons, the threefold classifications result in composites with size-varying CTP fields, the smallest composites being observed during summer. The variability in shape is rather weak, and much less pronounced than the one obtained by [*Chaboureau and Claud*, 2003] over the North Atlantic with zonally elongated or cyclonically tilted systems. This weak variability in the Mediterranean can be explained by the typical mesoscale or sub-synoptic size of the cloud systems. A systematic difference on the TLS field is found between the three classes of each season. Overall, the larger the TLS, the northernmost the class. This analysis shows that during winter, for about 30% of the cloud systems the dynamics is dominated by an upper PV anomaly. This rate decreases to 26% in spring and only 7% in autumn. However, it must be noted that, if the composite analysis is restricted to October, then 23% of the systems display a tropopause anomaly. In addition, these events in autumn are likely to be severe, since these are the only cases where the TLS values are larger than 220 K. This confirms the role of upper level troughs in the development of Mediterranean cloud systems, in agreement with *Trigo et al.* [2002]. Finally, in contrast, during summer, the forcing is very likely local, and according to the composite analysis, weakly related to PV anomaly.

[29] Moreover, the association between cloud systems and large scale circulation over the Atlantic during the cold season (from 15 October to 15 April) has been investigated. Two concepts have been considered to characterize this circulation: the NAO concept, and the weather regime concept. More systems are observed for negative NAO values, and this is especially true for the NE area and to a certain extent the SE area. For the period of interest, the number of detected systems was the largest during the Greenland Anticyclone regime. The Atlantic Ridge is also more favourable in terms of occurrence of cloud system, compared to the Zonal and Blocking regimes. In addition, during the Blocking regime, there is a larger fraction of small-scale systems (radius less than 400 km). Associated to each regime, preferential locations for cloud systems have been found. To our knowledge, this study is the first to

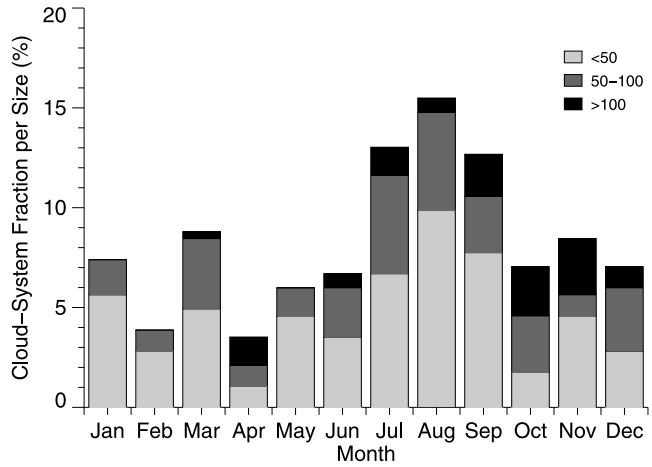


**Figure 13.** Monthly fraction of cloud systems per different categories of daily precipitation.

consider all Atlantic weather regimes and the characteristics of the Mediterranean cloud systems.

[30] Finally, this study has concentrated on the Alpine region in order to investigate the relationship between precipitation and the upper-level situation. It was found that severe precipitation events over this region are associated to a warm TLS anomaly upstream of the cyclone, showing once more the impact of the upper levels on the weather over this area. While this study consolidates previous ones, it also complements them especially in terms of establishing large scale configurations that are prone to developments over the Mediterranean Basin.

[31] These results have implications on the forecasting of Mediterranean storms: they show that the quality of the short-range forecasts (12–24 hours) can be improved by a better representation of the situation around the tropopause in the initial conditions for about one out of three cases. The potential of satellite sounder data for the study of storms is also illustrated. Further work will consist in considering the whole period of time during which TOVS data are available (since 1979).

[32] **Acknowledgments.** Retrievals were obtained from the Atmospheric Radiation Analysis group at LMD, through the NOAA/NASA TOVS Pathfinder (Path-B) program. The Alpine precipitation climatology comes from the MAP data center. This research has been supported by the Programme Atmosphère et Océan à Moyenne Echelle of the French Institut National des Sciences de l'Univers and the CYPRIM (CYclogenèse et PRécipitations Intenses en région Méditerranéenne) project funded by the French Research Ministry. Constructive comments by a reviewer are gratefully acknowledged.

## References

Alpert, P., B. U. Neeman, and Y. Say-El (1990a), Climatological analysis of Mediterranean cyclones using ECMWF data, *Tellus*, *42A*, 65–77.

Alpert, P., B. U. Neeman, and Y. Say-El (1990b), Intermonthly variability of cyclone tracks in the Mediterranean, *J. Clim.*, *3*, 1474–1478.

Ayrault, F., F. Lalaurette, A. Joly, and C. Loo (1995), North Atlantic ultra high frequency variability, *Tellus*, *47A*, 671–696.

Buzzi, A., and L. Foschini (2000), Mesoscale meteorological features associated with heavy precipitation in the Southern Alpine region, *Meteorol. Atmos. Phys.*, *72*(2–4), 131–146.

Cassou, C., L. Terray, J. W. Hurrell, and C. Deser (2004), North Atlantic winter climate regimes: Spatial asymmetry, stationarity with time, and oceanic forcing, *J. Clim.*, *17*, 1055–1068.

Chaboureau, J.-P., and C. Claud (2003), Observed variability of North Atlantic oceanic precipitating systems during winter, *J. Geophys. Res.*, *108*(D14), 4435, doi:10.1029/2002JD003343.

Chédin, A., N. A. Scott, C. Wahiche, and P. Moulinier (1985), The Improved Initialization Inversion Method: A high resolution physical method for temperature retrievals from the TIROS-N series, *J. Clim. Appl. Meteorol.*, *24*, 124–143.

Fourrié, N., C. Claud, J. Donnadille, J.-P. Cammas, B. Pouponneau, and N. A. Scott (2000), The use of TOVS observations for the identification of tropopause-level thermal anomalies, *Q. J. R. Meteorol. Soc.*, *126*, 1473–1494.

Fourrié, N., C. Claud, and A. Chédin (2003), On the depiction of upper-level precursors of the December 1999 storms from TOVS observations, *Weather Forecasting*, *18*, 417–430.

Frei, C., and C. Schär (1998), A precipitation climatology of the Alps from high-resolution rain-gauge observations, *Int. J. Climatol.*, *18*, 873–900.

Frei, C., J. H. Christensen, M. Déqué, D. Jacob, R. G. Jones, and P. L. Vidale (2003), Daily precipitation statistics in regional climate models: Evaluation and intercomparison for the European Alps, *J. Geophys. Res.*, *108*(D3), 4124, doi:10.1029/2002JD002287.

Hurrell, J. (1995), Decadal trends in the North Atlantic Oscillation: Regional temperature and precipitation, *Science*, *269*, 676–679.

Liniger, M. A., and H. C. Davies (2003), Substructure of a MAP streamer, *Q. J. R. Meteorol. Soc.*, *129*, 633–651.

Maheras, P., H. A. Flocas, I. Patrikas, and C. Anagnostopoulou (2001), A 40 year objective climatology of surface cyclones in the Mediterranean region: Spatial and temporal distribution, *Int. J. Climatol.*, *21*, 109–130.

Massacand, A. C., H. Wernli, and H. C. Davies (1998), Heavy precipitation on the Alpine southside: An upper-level precursor, *Geophys. Res. Lett.*, *25*, 1435–1438.

Petterssen, S. (1956), *Motion and Motion Systems*, vol. 1, *Weather and Forecasting*, 428 pp., McGraw-Hill, New York.

Picornell, M. A., A. Jansà, A. Genovés, and J. Campins (2001), Automated database of mesocyclones from the HIRLAM (INM)-0.5 analyses in the western Mediterranean, *Int. J. Climatol.*, *21*, 335–354.

Quadrelli, R., V. Pavan, and F. Molteni (2001), Wintertime variability of Mediterranean precipitation and its links with large-scale circulation anomalies, *Clim. Dyn.*, *17*, 457–466.

Scott, N. A., A. Chédin, R. Armante, J. Francis, C. J. Stubenrauch, J.-P. Chaboureau, F. Chevallier, C. Claud, and F. Chéruy (1999), Characteristics of the TOVS Pathfinder Path-B dataset, *Bull. Am. Meteorol. Soc.*, *80*, 2679–2702.

Stein, J., E. Richard, J.-P. Lafore, J.-P. Pinty, N. Asencio, and S. Cosma (2000), High-resolution non-hydrostatic simulations of flash-flood episodes with grid-nesting and ice-phase parameterization, *Meteorol. Atmos. Phys.*, *72*, 203–221.

Stubenrauch, C. J., A. Chédin, R. Armante, and N. A. Scott (1999a), Clouds as seen by infrared sounders (3I) and imagers (ISCCP), II, A new approach for cloud parameter determination in the 3I algorithms, *J. Clim.*, *12*, 2214–2223.

Stubenrauch, C. J., W. B. Rossow, F. Chéruy, A. Chédin, and N. A. Scott (1999b), Clouds as seen by infrared sounders (3I) and imagers (ISCCP), I, Evaluation of cloud parameters, *J. Clim.*, *12*, 2189–2213.

Trigo, I. F., T. D. Davies, and G. R. Bigg (1999), Objective climatology of cyclones in the Mediterranean region, *J. Clim.*, *12*, 1685–1696.

Trigo, I. F., G. R. Bigg, and T. D. Davies (2002), Climatology of cyclogenesis mechanisms in the Mediterranean, *Mon. Weather Rev.*, *130*, 549–569.

Trigo, R. M., I. F. Trigo, C. DaCamara, and T. J. Osborn (2004), Impact of the European winter blocking episodes from the NCEP/NCAR Reanalysis, *Clim. Dyn.*, *23*, 17–28, doi:10.1007/s00382-004-0410-4.

Vautard, R., B. Legras, and M. Déqué (1988), On the source of midlatitude low-frequency variability. Part I: A statistical approach to persistence, *J. Atmos. Sci.*, *45*, 2811–2844.

J.-P. Chaboureau, Laboratoire d'Aérologie, Observatoire Midi-Pyrénées, 14 avenue Belin, 31400 Toulouse, France. (jean-pierre.chaboureau@aero.obs-mip.fr)

C. Claud, Laboratoire de Météorologie Dynamique/IPSL, École Polytechnique, 91128 Palaiseau Cedex, France. (chantal.claud@lmd.polytechnique.fr)